Princeton Plasma Physics Laboratory

PPPL- 4963

PPPL- 4963

Influence of Emitted Electrons Transiting Between Surfaces on Plasma-Surface Interaction

M.D. Capanell and H. Wang

DECEMBER, 2013

Prepared for the U.S. Department of Energy under Contract DE-AC02-09CH11466.

Princeton Plasma Physics Laboratory
Report Disclaimers

Full Legal Disclaimer

Trademark Disclaimer

PPPL Report Availability

Princeton Plasma Physics Laboratory:

http://www.pppl.gov/techreports.cfm

Office of Scientific and Technical Information (OSTI):

http://www.osti.gov/bridge

Related Links:

U.S. Department of Energy

Office of Scientific and Technical Information

Fusion Links

Influence of Emitted Electrons Transiting Between Surfaces on Plasma-Surface Interaction

M.D. Campanell[1], H. Wang[2]

[1]*Princeton Plasma Physics Laboratory, Princeton University, Princeton, New Jersey 08543, USA*
[2]*Beijing University of Aeronautics and Astronautics, Beijing, China*

Emitted electrons are accelerated back into the plasma by the sheath. If their mean free path is large, they can propagate directly to another surface without suffering collisions. We analyze effects of "transit" on plasma-surface interaction. When transit occurs, surfaces exchanging electrons are intricately coupled. All surfaces float more negatively than they would if the emission collisionally remixed with the bulk plasma. Asymmetries of the system drive a net "transit current" between the surfaces, which influences their potential difference. The larger the initial energy spread of the emitted electrons, the larger the potential difference.

Electron emission from surfaces is important in many plasma applications. Most theoretical models[1,2,3,4,5] and particle simulation studies[6,7,8] of plasma-surface interaction (PSI) with emission treat a plasma source contacting *one* wall; the influx of electrons to the wall comes only from thermal plasma electrons. But plasmas are often surrounded by surfaces. So in practice is important to consider whether emitted electrons transit from surface to surface and how this could affect PSI globally.

Although emitted electrons have small initial velocity, they get accelerated away from the surface by the sheath to a much larger velocity. Probes can detect secondary electron emission (SEE) propagating deep into a plasma as a directed beam[9]. Naturally, secondaries should have enough energy to overcome a sheath of amplitude equal to or smaller than the one they came from. Thus it is plausible in general that some secondaries will reach a surface unless the collisional mean free path is much smaller than the distance to travel. We will focus on SEE "transit" in this work, though transit is possible for any type of emission. For example, direct flight of electrons from cathode to anode occurs in Knudsen thermionic converters[10].

Observations of secondaries transiting to surfaces can be found in the recent literature. SEE from the lunar surface was detected reaching a spacecraft in orbit[11]. At low operating pressure, energetic secondaries from plasma immersion ion implantation targets generate x-rays upon impacting the surrounding chamber walls[12]. Hall thruster (HT) simulations show secondaries crossing from each channel wall to the other[13,14,15]. In simulations of a low pressure hollow cathode discharge, some trajectories of secondaries from the cylinder appear to reach the cylinder again, see Fig. 2(f) of Ref. 16. In most real systems, it may be difficult to directly prove that secondaries reach surfaces especially if they have low impact energy or if the surfaces are dielectrics. But in light of the energy conservation argument and the diverse examples above, transit is likely a common phenomenon.

A key consequence of transit is that it alters flux balance at the plasma-facing surfaces. While a plasma-sheath model for a planar plasma bounded by walls with equal electron-induced SEE coefficients accounting for transit was treated by Ahedo and Parra[17], in that configuration, the two transiting SEE "beams" cancel due to the symmetry.

If a system is asymmetric, some interesting complexities arise because the transiting beams will be unequal. For example, if one wall has a larger SEE yield (Fig. 1(a)) or larger surface area (Fig. 1(b)) than the opposite wall, it will emit more electrons. Also, even if two interacting walls emit the same outflux, the transiting beams will be unequal if some secondaries from one wall cannot reach the other wall due to a potential difference from biasing (Fig. 1(c)), or a magnetic mirror force (Fig. 1(d)).

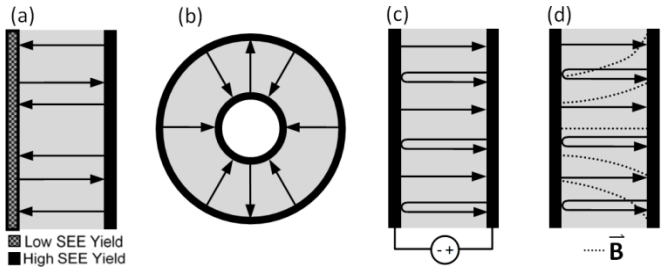

FIG. 1. Examples of asymmetries that cause surfaces to exchange secondaries at unequal rates. Arrows show representative trajectories of secondaries through the gray plasma region.

In this letter, we analyze effects of transit on PSI with general theory and simulated examples. First we simulate a planar plasma between floating walls with different SEE yields using the electrostatic direct implicit particle-in-cell code[18] (Fig. 2). The main control parameters in EDIPIC are plasma width H, (xenon) plasma density n_p, neutral atom density n_n, magnitudes of uniform background fields **E** and **B**, and turbulent collision frequency ν_{turb}. Electrons move in response to the E×B field, the plasma's self-generated potential $\varphi(x)$, and collisions. Collisions include elastic and inelastic scatters with neutral atoms, Coulomb interaction, and turbulent collisions. Turbulent collisions (random scatters of the velocity component normal to **B**) simulate anomalous transport in E×B fields. The right wall emission models boron nitride ceramics. In the energy range of interest, the total SEE yield vs. impact energy is roughly

$\gamma_{BNC}(\varepsilon) \approx 0.17\varepsilon^{1/2}$ (ε in eV). The yield includes (a) cold "true secondaries" emitted with a thermal distribution (T_{emit} = 2eV) *and* (b) reflected and backscattered incident electrons. Here, the particular wall materials are less important than asymmetry of materials. We introduce asymmetry by setting the yield function of the left wall to $\beta\gamma_{BNC}$, with β an adjustable factor.

Past EDIPIC simulations modeling the PPPL HT acceleration region revealed important kinetic effects not captured by fluid theories including temperature anisotropy, loss cone depletion and SEE beam-driven transport[13,14,18]. These results have been applied to explain experimental measurements[19]. All past papers using this simulation configuration treated a symmetric system.

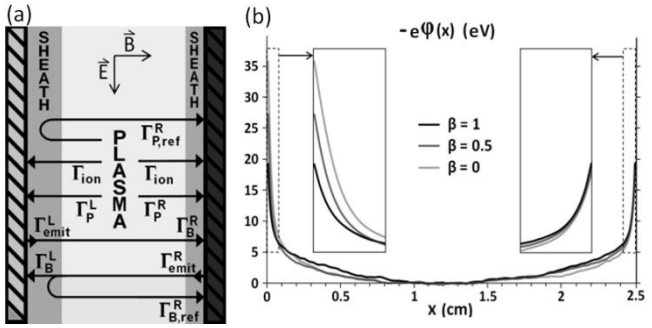

FIG. 2. (a) The simulated system. Wall particle flux components that exist when $\Phi_L > \Phi_R$ are sketched. (b) Potential energy of an electron relative to the extremum in the plasma interior.

Here we present a simulation with H = 2.5 cm, $n_p = 5 \times 10^{10}$ cm^{-3}, $n_n = 10^{12}$ cm^{-3}, E = 100V/cm, B = 100G, and $\nu_{turb} = 2.8 \times 10^6$ s^{-1}. The resulting plasma is anisotropic due to low collisionality. Approximate electron temperatures parallel $T_{//}$ = 51eV and normal T_x = 7eV to the walls are computed from the mean kinetic energy of electrons near the midplane in each direction. Initially, β = 1. Since the system is symmetric, the potential difference between the plasma interior and each wall is equal, $\Phi_R \equiv -\varphi(x=H) = \Phi_L \equiv -\varphi(x=0) = \Phi_{symm}$ = 19V, see Fig. 2(b). Electrons with energy normal to the walls $w_x \equiv \frac{1}{2}m_e v_x^2 - e\varphi(x)$ below $e\Phi_{symm}$ are trapped regardless of their parallel energy $w_{//}$. The plasma electron flux to each wall (Γ_P) comes from initially trapped electrons with *total* energy $w = w_{//} + w_x$ exceeding $e\Phi_{symm}$ that get scattered into the loss cone ($w_x > e\Phi_{symm}$). SEE from the other wall produces "beam flux" (Γ_B). More details on the physics behind the plasma properties, $T_{//}$, T_x, Φ_{symm} and their dependence on control parameters appear in Ref. 14.

There is another flux Γ_{wc} from "weakly confined electrons". Field fluctuations from plasma waves nudge electrons with w_x slightly below $e\Phi_{symm}$ into the loss cone. The fluctuations also cause some beam electrons to become trapped. In most situations in quasisteady state, the rate of electrons entering and leaving the loss cone "diffusively" are practically equal; for flux balance one can equivalently assume no beam electrons get trapped this way and Γ_{wc} does not exist. Then since the collisional mean free path is large enough that secondaries rarely suffer collisions, one can assume the emitted beams transit fully and cancel in the flux balance. These assumptions are justified because in Fig. 3 when $\beta = 1$, $\Gamma_P = \Gamma_{ion}$ at each wall.

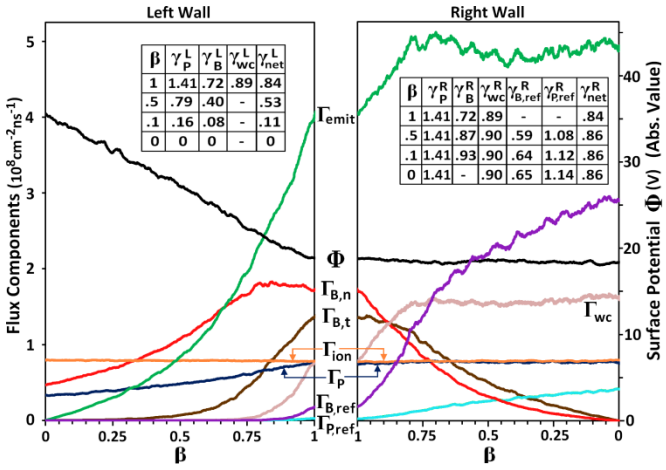

FIG. 3. (color online) Plot of the fluxes and Φ at each wall vs. β. The beam flux Γ_B is separated by true ($\Gamma_{B,t}$) and non-true ($\Gamma_{B,n}$) parts. The tables give the net SEE coefficient γ_{net} and partial coefficient of each flux component for several β. A hyphen means no coefficient exists because the flux component is ≈ 0.

Now β is varied quasistatically from 1 to 0 in the simulation. The plasma properties and EVDF are unaffected, so the variation of fluxes and wall potentials is due only to the wall material asymmetry. In Fig. 2(b), $\varphi(x)$ for three β values is plotted. We see reducing β causes Φ_L to increase. Now some emission from the right wall Γ^R_{emit} is unable to overcome the left sheath. Hence in Fig. 3 as Φ_L increases, Γ^L_B decreases; the suppressed electrons reflect back through the plasma to the right wall, producing a "reflected beam" $\Gamma^R_{B,ref}$. Similarly, as Φ_L increases, Γ^L_P decreases. Now plasma electrons that approach the left wall with $e\Phi_R < w_x < e\Phi_L$ reflect off the left sheath and then hit the right wall ($\Gamma^R_{P,ref}$).

To show implications of transit, we will analyze PSI in the simulated plasma slab and contrast to the analogous result for PSI without transit. At first, it may seem necessary to theoretically calculate all flux components vs. β at each wall in Fig. 3. This would be very complicated as each component induces SEE at a different average rate (see the "partial SEE coefficient" tables). The destination of each secondary, its impact energy and SEE induced depends on its emission energy, the (initially unknown) potential difference $\Delta\Phi \equiv \Phi_L - \Phi_R$, and β. But despite the intricate coupling of the walls, general conclusions about flux balance follow from the "transit principle": in the low collisionality limit, all emitted electrons are recaptured at a surface. So emission produces no net electron flow into the plasma globally.

The condition for global charge balance is thus that the total flux to all surfaces from plasma electrons (determined by the surface potentials) must add up to the total ion flux. The emitted and incident beams add up to zero by the transit

principle. In the slab, the ion flux Γ_{ion} at each wall is equal and fixed by Bohm's criterion. Because $\Phi_L \geq \Phi_R$ when $\beta \leq 1$ (to be proven later) we have,

$$\Gamma_P^R(\Phi_R) + \Gamma_{P,ref}^R(\Phi_L, \Phi_R) + \Gamma_P^L(\Phi_L) = 2\Gamma_{ion} \quad (1)$$

Note the plasma electrons approaching the left wall with $w_x > e\Phi_R$ will ultimately hit either the left wall (if $w_x > e\Phi_L$) or right wall (if $e\Phi_L > w_x > e\Phi_R$), producing the same total flux Γ_P^R. That is, $\Gamma_P^R = \Gamma_{P,ref}^R + \Gamma_P^L$. It follows,

$$\Gamma_P^R(\Phi_R) = \Gamma_{ion} \quad (2)$$

Eq. (2) shows the right wall must float at fixed potential $\Phi_R = \Phi_0$, where Φ_0 denotes the potential a wall floats at if there is no SEE! Although Ref. [14] showed the potentials at both walls were insensitive to SEE in the symmetric system where the beams cancel ($\Phi_{symm} = \Phi_0$), it is surprising that Φ_R remains almost constant for all $\beta < 1$ in Fig. 3, even as many right wall flux components and coefficients vary. Only Φ_L varies with β because $\Delta\Phi$ is governed by the unequal transiting beams. Since nearly all secondaries reach a wall, the *net* electron flux to each wall is expressible as,

$$\Gamma_{e,net}^L = \Gamma_P^L + \Gamma_B^L - \Gamma_B^R \quad (3)$$

$$\Gamma_{e,net}^R = \Gamma_P^R + \Gamma_{P,ref}^R + \Gamma_B^R - \Gamma_B^L \quad (4)$$

Since the walls float, $\Gamma_{e,net}^R = \Gamma_{ion} = \Gamma_{e,net}^L$. Equating (3) with (4), using $\Gamma_P^R = \Gamma_{P,ref}^R + \Gamma_P^L$, gives a floating condition,

$$\Gamma_{P,ref}^R(\Phi_L, \Phi_0) = J_{trans}(\Phi_L, \Phi_0) \quad (5)$$

where $J_{trans} \equiv \Gamma_B^L - \Gamma_B^R$ is the net "transit current" density exchanged by the walls. If the plasma EVDF is known, Φ_0 from (2) is calculable and then $\Gamma_{P,ref}^R$ is known as a function of Φ_L. But solving for Φ_L in (5) exactly is formidable because calculating J_{trans} vs. Φ_L requires calculating the energy distribution of beams self-consistently with Φ_L.

For the gist of how Φ_L is determined, first suppose $\Delta\Phi = 0$. Then $\Gamma_{P,ref}^R = 0$, and both beams transit fully to the other wall; $\Gamma_B^L = \Gamma_{emit}^R$, $\Gamma_B^R = \Gamma_{emit}^L$. The outflux Γ_{emit} comes from SEE produced by impacting plasma and beam electrons:

$$\begin{aligned} \Gamma_B^L &= \Gamma_{emit}^R = \gamma_P^R \Gamma_P^R + \gamma_B^R \Gamma_B^R \\ \Gamma_B^R &= \Gamma_{emit}^L = \gamma_P^L \Gamma_P^L + \gamma_B^L \Gamma_B^L \end{aligned} \quad (6)$$

The SEE coefficient of plasma electrons γ_P depends on plasma temperature and surface material; it can exceed unity in laboratory[20] and space[21] applications. Generally the SEE coefficient of beam electrons γ_B is less than γ_P, but not negligible. Non-true SEE ensures $\gamma_B > 0$. E×B drift energy gained parallel to the walls in transit also raises γ_B. Basically, beam coefficients amplify the beams. For $\Phi_L = \Phi_R = \Phi_0$, $\Gamma_P^L = \Gamma_P^R = \Gamma_{ion}$. Plugging this into (6), we can solve for Γ_B^L and Γ_B^R; taking their difference gives the transit current that would flow if the potential difference were zero $J_{trans}^{\Delta\Phi=0}$,

$$J_{trans}^{\Delta\Phi=0} = \Gamma_{ion} \frac{\gamma_P^R(1-\gamma_B^L) - \gamma_P^L(1-\gamma_B^R)}{1-\gamma_B^R\gamma_B^L} \quad (7)$$

If $\beta < 1$, then $\gamma_P^R > \gamma_P^L$ and $\gamma_B^R > \gamma_B^L$. It follows $J_{trans}^{\Delta\Phi=0} > 0$. So to maintain (5), the wall potentials cannot be equal as $\Gamma_{P,ref}^R$ would be zero. Since the wall with smaller Φ must float at Φ_0 for global charge balance, Φ_L must increase above Φ_0. This increases $\Gamma_{P,ref}^R$ *and* decreases J_{trans} below $J_{trans}^{\Delta\Phi=0}$ as some emission from the right wall is sent back to the right wall ($\Gamma_{B,ref}^R$) producing no current. Since $J_{trans} \to 0$ for large Φ_L, a solution to (5) with $\Phi_L > \Phi_0$ exists by the intermediate value theorem. The smaller β is, the larger $J_{trans}^{\Delta\Phi=0}$ is, and the further Φ_L must exceed Φ_0 (Fig. 3).

The result that a wall floats at $\Phi > \Phi_0$ violates familiar PSI principles. For PSI in a slab without transit, there are no beam influxes. Each wall independently satisfies the floating condition for one-wall models[1-7]; $\Gamma_P(\Phi) = \Gamma_{ion}/(1-\gamma_P)$. If both walls emit, then both have $\Gamma_P > \Gamma_{ion}$ and $\Phi < \Phi_0$. For a Maxwellian EVDF and xenon ions, Φ drops from $e\Phi_0 \approx 5T_e$ for $\gamma_P = 0$ to $e\Phi \approx T_e$ for $\gamma_P \geq 1$ when the sheath is space charge saturated[1,3]. With transit, assuming $\gamma_B^R,\ \gamma_B^L < 1$, neither sheath becomes saturated (Fig. 2(b)) even when γ_P^R and/or γ_P^L exceed unity (Fig. 3); $\gamma_{net} < 1$ at both walls. Also since the global plasma electron influx ($2\Gam_{ion}$ via (1)) is independent of emission, the plasma energy flux does not increase with emission yield as it does for one-wall PSI.

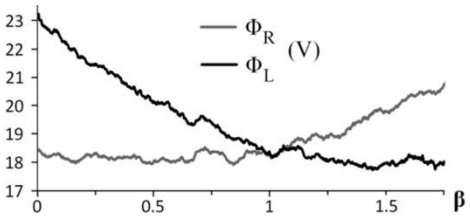

FIG. 4. Simulation performed with the same total SEE yield function γ_{BNC}, except all secondaries are true.

Non-true secondaries play an important role in transit. Notice in Fig. 3 as Φ_L increases, the true part of the left wall beam flux $\Gamma_{B,t}^L$ decreases faster than the non-true part $\Gamma_{B,n}^L$ because non-true secondaries have a broader range of emission energies. If all SEE was "cold", then $\Delta\Phi$ could never exceed a few T_{emit} or else Γ_B^L would be zero, giving the two sides of (5) opposite signs. In Fig. 4, a simulation is run to produce a plasma with the same properties, but now the non-true part of the SEE yield is replaced with true SEE. In this run as β is varied from 0 to 1.75, $|\Delta\Phi|$ never exceeds 5V (compare to $\Delta\Phi = 18$V in Fig. 3 when $\beta = 0$). Fig. 4 also shows an interesting transition occurs when β crosses 1. Because $J_{trans}^{\Delta\Phi=0}$ changes sign, Φ_L becomes roughly fixed at Φ_0; then further increasing the emission yield of the left wall strengthens the *right* sheath!

Another key asymmetry that can drive transit currents is surface geometry. Consider a uniform annular plasma with inner wall radius R_1 and outer wall radius R_2 (Fig. 1(b)). Assume the Debye length is small and the walls have equal γ_p. It turns out the walls will float at equal potentials only if all the SEE collisionally thermalizes. Otherwise, the potentials must differ owing to a transit current that arises because the *total* emission from a surface is proportional to surface area. In the zero thermalization limit, $|J_{trans}^{\Delta\Phi=0}| = \gamma_p\Gamma_{ion}(R_2\text{-}R_1)/R_1$ at the inner wall (if $\gamma_b = 0$).

Let us consider transit between mutually biased surfaces (Fig. 1(c)). Now $\Delta\Phi$ is fixed and the current is the unknown. We model the same plasma system as earlier, with $\beta = 1$, and vary $\Delta\Phi$. Because the transit principle still applies, we can determine Φ_L and Φ_R using the same charge balance constraint. The wall with less negative potential must have $\Phi = \Phi_0$. So the other wall has $\Phi = \Phi_0 + |\Delta\Phi|$.

Although the wall materials are symmetric, the sheath asymmetry from biasing drives transit current which influences the current-voltage trace of the walls. In Fig. 5, we plot the net electron current $J_{net}^R = \Gamma_{e,net}^R - \Gamma_{ion}$ vs. $\Delta\Phi$. The current from just the plasma $J_P^R = \Gamma_P^R + \Gamma_{P,ref}^R - \Gamma_{ion}$ is also plotted. The function $J_P^R(\Delta\Phi)$ resembles a double probe trace, saturating at $\pm\Gamma_{ion}$ for large bias. The difference between J_P^R and J_{net}^R is J_{trans}. J_{net}^R has a large slope near the origin because J_{trans} changes sharply, as a few volt bias stops most true secondaries from one wall from reaching the other. $|J_{net}^R|$ actually exceeds Γ_{ion} for a range of $\Delta\Phi$, but still approaches $|\Gamma_{ion}|$ for large bias, making the I-V trace nonmonotonic. Note if the wall materials are asymmetric, the trace becomes more irregular than Fig. 5. $J_{trans}(\Delta\Phi)$ and $J_{net}(\Delta\Phi)$ are not odd functions anymore, and surprisingly there is nonzero current for zero bias ($J_{trans}^{\Delta\Phi=0} \neq 0$ in (7)).

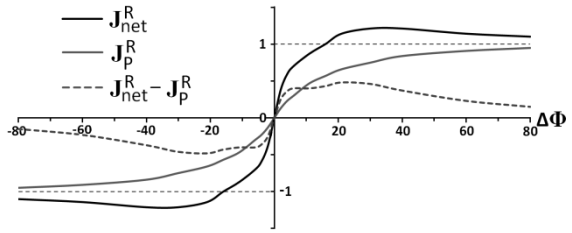

FIG. 5. Right wall electron current vs. $\Delta\Phi$, in units of Γ_{ion}.

We will briefly discuss some applications where the concepts introduced in this letter may apply. A recent review of dust grain charging reports evidence that secondaries from grains in dusty plasmas are captured by nearby grains when the grain concentration is high[22], making grains charge more negatively. Since it is known that the SEE yield of grains varies sharply with size[22], transit currents between small grains and large grains driven by surface area and SEE yield asymmetries could also affect grain potentials.

Transit is expected to occur in HT's[14,19]. There is experimental evidence of asymmetric wall materials influencing radial potential profiles[23]. Other asymmetries that can affect transit current in HT's are annular geometry and the 1/r magnetic field variation that mirror reflects part of the emission from the outer wall[15], c.f. Fig. 1(b,d).

SEE and photoelectrons from spacecraft are predicted to be recaptured by its other surfaces in certain situations[21]. Differential charging asymmetries arise from sunlight exposure on part of the craft, different component materials, sizes or shapes, *etc.*[21] In these conditions, nonzero currents will flow between surfaces exchanging electrons.

Ion-induced SEE is important for RF discharges. Recent work shows that asymmetric electrode materials can drive substantial dc bias across geometrically symmetric capacitively coupled plasmas due to the unequal SEE fluxes[24]. Ref. [24] studied a collisional regime where the SEE is roughly a constant outflux. Further complexities may arise in low pressure RF discharges, where secondaries propagate across the plasma[25]. In this regime they can impact the other electrode or reflect off the sheath, eventually reaching either electrode depending how the sheath potentials oscillate. Thus transit can make the net flux from SEE at RF discharge electrodes exhibit a complex time dependence.

Overall, the physics of PSI with emission differs when the emitted electrons reach surfaces compared to when they collisionally thermalize in the plasma. Emission is no longer a local correction to the flux balance at each surface but a global problem. The quantitative effects of transit will vary for each system. Generally, transit reduces the global loss rate of plasma electrons, thereby making potentials of interacting surfaces more negative. Also, if surfaces exchange electrons at unequal rates due to asymmetric conditions; the resulting "transit current" plays a key role in establishing their potential difference.

ACKNOWLEDGEMENT

This work was supported by the U.S. Department of Energy under Contract Number DE-AC02-09CH11466.

[1]G.D. Hobbs and J.A. Wesson, Plasma Phys. **9**, 85 (1967).
[2]V.I. Sizonenko, Sov. Phys. Tech. Phys. **26**, 1345 (1981).
[3]J. Seon, E. Lee, W. Choe and H. Lee, Curr. Appl. Phys. **12**, 663 (2012).
[4]C.A. Ordonez, Phys. Fluids B **4**, 778 (1992).
[5]J.P. Sheehan *et. al.*, in International Conference on Plasma Science, Edinburgh, UK, 2012.
[6]L. A. Schwager, Phys. Fluids B **5**, 631 (1993).
[7]F. Taccogna, S. Longo and M. Capitelli, Phys. Plasmas **11**, 1220 (2004).
[8]F. Zhang, D. Yu, Y. Ding and H. Li, Appl. Phys. Lett. **98**, 111501, (2011).
[9]P.G. Coakley and N. Hershkowitz, Phys. Lett. A **78**, 145 (1980).
[10]V.I. Sitnov, A.Ya. Énder and E.V. Yakovlev, Technical Physics **44**, 373 (1999).
[11]J.S. Halekas *et. al*. Planetary and Space Science **57**, 78 (2009).
[12]K. Nakamura, M. Tanaka and H. Sugai, Surface and Coatings Technology **169**, 57 (2003).
[13]D. Sydorenko, *et al.*, Phys. Plasmas **13**, 014501 (2006).

[14]I.D. Kaganovich, Y. Raitses, D. Sydorenko and A. Smolyakov, Phys. Plasmas **14**, 057104 (2007).
[15]F. Taccogna, S. Longo, M. Capitelli, and R. Schneider, Contrib. Plasma Phys. **48**, 375 (2008).
[16]G.J. Kim, F. Iza and J.K. Lee, J. Phys. D. **39**, 4386 (2006).
[17]E. Ahedo and F.I. Parra, Phys. Plasmas **12**, 073503 (2005).
[18]D. Sydorenko, Ph.D. Thesis, U. of Saskatchewan, 2006.
[19]Y. Raitses *et al.*, IEEE Trans. Plasma Science, **39**, 4, (2011).
[20]C.A. Ordonez and R.E. Peterkin, J. Appl. Phys. **79**, 2270 (1996).
[21]E. C. Whipple, Rep. Prog. Phys. **44**, 1198 (1981).
[22]J. Pavlů, J. Šafránovká, Z. Němeček, and I. Richterová, Contrib. Plasma Phys. **49**, 169 (2009).
[23]Y. Raitses, D. Staack and N.J. Fisch, IEEE Trans. Plasma Science **36**, 1202 (2008).
[24] T. Lafleur, P. Chabert and J.P. Booth, J. Phys. D: Appl. Phys. **46**, 135201 (2013).
[25] R. Flohr and A. Piel, Phys. Rev. Lett. **70**, 1108 (1993).

The Princeton Plasma Physics Laboratory is operated
by Princeton University under contract
with the U.S. Department of Energy.

Information Services
Princeton Plasma Physics Laboratory
P.O. Box 451
Princeton, NJ 08543

Phone: 609-243-2245
Fax: 609-243-2751
e-mail: pppl_info@pppl.gov
Internet Address: http://www.pppl.gov